

Dopamine uptake sites in the striatum are distributed differentially in striosome and matrix compartments

(nigrostriatal/ligand binding/mazindol/1-methyl-4-phenyl-1,2,3,6-tetrahydropyridine/cocaine)

ANN M. GRAYBIEL* AND ROSARIO MORATALLA

Department of Brain and Cognitive Sciences, E25-618, Massachusetts Institute of Technology, 45 Carleton Street, Cambridge, MA 02139

Contributed by Ann M. Graybiel, August 16, 1989

ABSTRACT A major mechanism of neurotransmitter inactivation at catecholaminergic synapses is reuptake of released transmitter at high-affinity uptake sites on presynaptic terminals. We have analyzed the anatomical distribution of site-selective ligand binding for dopamine uptake sites in the striatum of rat, cat, and monkey. We report here that desipramine-sensitive [³H]mazindol binding sites have highly heterogeneous distributions in the dorsal and the ventral striatum. In the caudate nucleus of cat and monkey, [³H]mazindol binding observes striosomal ordering, being reduced in striosomes and heightened in the extrastriosomal matrix. Some local heterogeneity appears in the ventral caudoputamen of the rat. Different subdivisions of the nucleus accumbens also have different binding levels. These findings suggest that some functional effects of psychoactive drugs, such as cocaine, that bind to the dopamine-uptake complex could be related to the distribution of these specific uptake sites. The findings also raise the possibility that these distributions could result in selective neuronal vulnerability to neurotoxins, such as 1-methyl-4-phenylpyridine (MPP⁺), that depend on the dopamine-uptake complex for entry into neurons.

A number of powerful psychoactive drugs, including cocaine and amphetamine, bind to sites on the presynaptic uptake complex that constitutes a major means for neurotransmitter inactivation at catecholaminergic synapses (1-3). Catecholamine-uptake sites are also potential conduits for the entry of neurotoxins and neurotoxin precursors into catecholaminergic synapses. This route is of special interest in relation to the drug-induced parkinsonian syndrome elicited by 1-methyl-4-phenyl-1,2,3,6-tetrahydropyridine (MPTP) (4-6). The toxic oxidative metabolite of MPTP, 1-methyl-4-phenylpyridine (MPP⁺), is thought to enter catecholamine-containing neurons by means of the uptake transport mechanism (7, 8). Blockade of dopaminergic and noradrenergic uptake sites with specific blockers prevents the toxic effects of MPTP administration on dopaminergic and noradrenergic neurons (9-12). The precise distribution of high-affinity uptake sites within the catecholaminergic systems of the brain is thus important not only in relation to the normal physiology of these pathways but also in relation to the selective effects of drugs and environmental toxins on catecholaminergic function.

In the experiments reported here we used *in vitro* ligand-binding autoradiography with the radiolabeled catecholamine uptake blocker [³H]mazindol in the presence of desipramine (13, 14) to study the detailed distribution of high-affinity dopamine uptake sites in the striatum. The results suggest that in cat and monkey there are notable differences in the amounts of [³H]mazindol binding in the two main tissue compartments of the dorsal striatum, the striosomes and the

extrastriosomal matrix (15); and they suggest that different subdivisions of the ventral striatum in rat, cat, and monkey are also characterized by different levels of binding. These differential anatomical distributions may help to account for some of the functional and toxicological selectivities of drugs acting on the mesostriatal system.

MATERIALS AND METHODS

Brains were removed from one cat, two rats, (one Sprague-Dawley; one Wistar), one squirrel monkey, and one cynomolgus monkey after induction of terminal anaesthesia with sodium pentobarbital (Nembutal). Blocks containing the striatum were frozen in pulverized dry ice and were cut transversely at 20 μ m on a cryostat immediately or after brief storage at -70°C. Sections cut at -12°C and thaw-mounted onto "subbed" slides were dried at 4°C in a desiccator under vacuum, stored at -20°C for at least 2 weeks, and then incubated according to the protocols of O'Dell and Marshall (14) and Javitch *et al.* (13). For autoradiographic studies, sections were preincubated in 50 mM Tris-HCl (pH 7.9) containing 120 mM NaCl and 5 mM KCl at 4°C (5 min), then incubated in 50 mM Tris-HCl (pH 7.9) containing 300 mM NaCl, 5 mM KCl, either 2 nM or 15 nM [³H]mazindol (15 Ci/mmol; 1 Ci = 37 GBq; DuPont/NEN), and 0.3 μ M desipramine (40 min, 4°C), washed in fresh buffer (two 3-min washes, 4°C), and briefly rinsed in distilled water (10 sec, 4°C). Sections were dried under a cool airstream and applied to ³H-sensitive film (Hyperfilm, Amersham) for 3 weeks at -20°C. Control sections were prepared in parallel by addition of 1 μ M unlabeled mazindol or 30 μ M benztropine to the incubation medium. Controls were applied to each film along with tritium standards (³H]Micro-scales; Amersham). After autoradiographic exposure, selected sections were stained for acetylcholinesterase (AChE) or (for squirrel monkey) butyrylcholinesterase by slightly modified Geneser-Jensen and Blackstad protocols (15, 16) to permit detection of striosomes. Densitometry was carried out with a BIOCUM 200 computer system (Les Ulis, France). A standard sampling zone was superimposed under cursor control on video images of [³H]mazindol-poor zones and on adjacent [³H]mazindol-rich tissue identified in films of sections through the cat's caudate nucleus. Relative grey-level values were calculated for all regions sampled, and values were converted to nCi/mg of tissue (equivalent weight) with BIOCUM software using the [³H]Micro-scales. Mean levels of [³H]mazindol binding were calculated for summed regions inside and outside the [³H]mazindol-labeled compartments, and values were compared by Student's *t* test (2-tailed).

The publication costs of this article were defrayed in part by page charge payment. This article must therefore be hereby marked "advertisement" in accordance with 18 U.S.C. §1734 solely to indicate this fact.

Abbreviations: MPTP, 1-methyl-4-phenyl-1,2,3,6-tetrahydropyridine; AChE, acetylcholinesterase.

*To whom reprint requests should be addressed.

RESULTS

Dense [^3H]mazindol binding appeared in the striatum in all brains under normal incubation conditions and binding was absent in control sections. At mid-anterior levels through the cat's striatum, binding in the caudate nucleus was highly patterned, with circumscribed zones of relatively reduced binding punctuating otherwise densely labeled fields (Fig. 1A). Most of the [^3H]mazindol-poor zones could be identified as striosomes when the autoradiographic images were compared with AChE staining patterns developed from the same sections: the shapes and positions of the zones of low [^3H]mazindol binding matched those of the AChE-poor zones (Fig. 1). Even in single films, the degree of patterning of [^3H]mazindol was not equivalent at all anteroposterior and dorsoventral levels of the striatum. Binding tended to be more homogeneous caudally and dorsolaterally in the caudate nucleus, as did the AChE staining, and little patterning was visible in the putamen. Occasionally, regions of relatively heightened binding were evident. Correspondents for these were not identified in AChE stains.

Pockets of reduced [^3H]mazindol binding were also observed in the caudate nucleus of the squirrel monkey (Fig. 2) and cynomolgus monkey (Fig. 3), but the autoradiography was not as crisp as in the cat and not every AChE-poor striosome could be matched to a [^3H]mazindol-poor zone. Even so, it was possible in both primate species to confirm correspondence of many [^3H]mazindol-poor zones with striosomes identified histochemically in the same sections after autoradiography. Patterns of binding were quite diffuse in the putamen. No clear patchiness in [^3H]mazindol binding was evident in the central and dorsal regions of rat's caudoputamen, but ventrally in the caudoputamen some zones of low binding did appear.

Densitometry performed for the cat's caudate nucleus (Table 1) indicated that the mean binding in the [^3H]mazindol-poor zones was 51.23% of the mean binding in adjacent matrix tissue ($n = 63$ sampled zones in four sections).

There were marked differences in the intensity of binding in different parts of the nucleus accumbens. As shown in Fig. 4 for the cat, binding was dense rostralaterally but was very weak caudally and medially. Comparable variations were

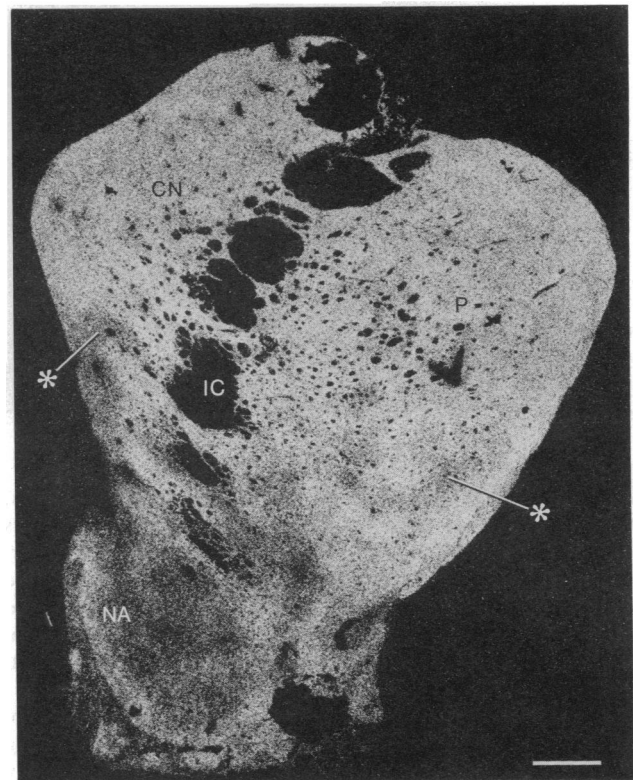


FIG. 2. [^3H]Mazindol binding in striatum of squirrel monkey. Zones of reduced binding in the caudate nucleus (matching histochemically identified striosomes, data not shown) were mainly found in the ventral half of the nucleus (example at asterisk). Slight heterogeneity is also evident in binding in putamen (see asterisk), and subdivision-specific variations in binding are present in the nucleus accumbens-ventral striatum. From case SQDAR-4. Photograph was printed directly from autoradiographic film. CN, caudate nucleus; P, putamen; IC, internal capsule; NA, nucleus accumbens. (Bar = 1 mm.)

present in the monkeys, and in the rat the "shell" subdivision of the nucleus accumbens (17) had much reduced binding compared to that of the core subdivision.

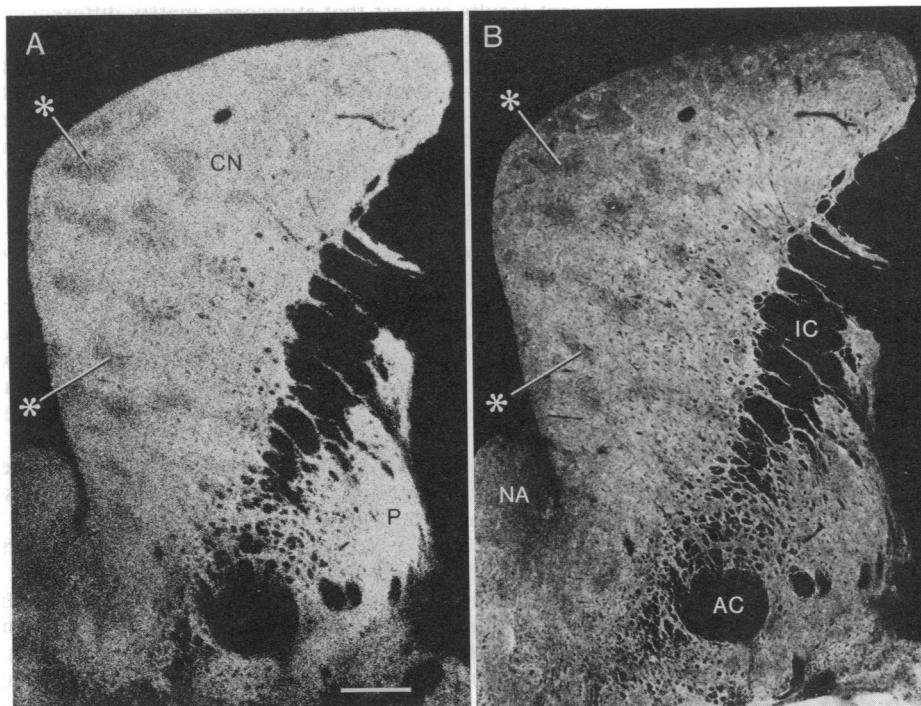


FIG. 1. [^3H]Mazindol binding (A) and AChE activity (B) in serial transverse sections through the striatum of an adult cat. Photograph in A was directly printed from film; photograph in B is negative-image print. Prominent patches of reduced [^3H]mazindol binding appear in the central part of the caudate nucleus. These correspond to the AChE-poor striosomes visible in B (examples at asterisks). From case CDAR-12. CN, caudate nucleus; P, putamen; IC, internal capsule; AC, anterior commissure; NA, nucleus accumbens. (Bar = 1 mm.)

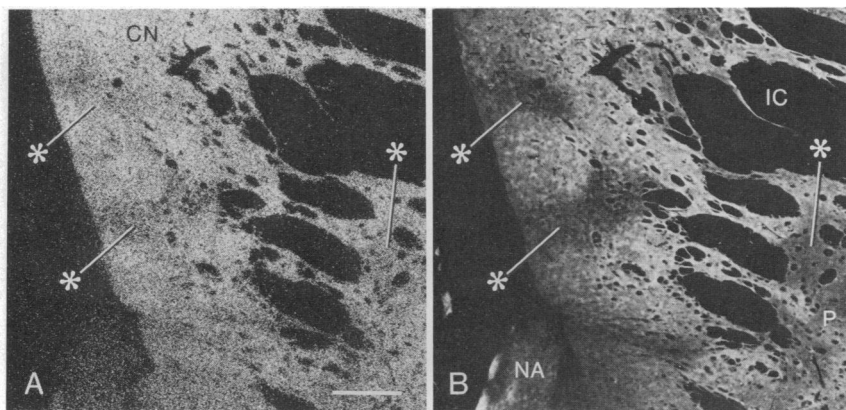


FIG. 3. Sector of medial caudate nucleus of cynomolgus monkey illustrating correspondence (see asterisks) between zones of reduced $[^3\text{H}]$ mazindol binding (A) and zones of reduced AChE-staining (B). Note similarity in size and shape of zones in the two images. (A) Printed directly from film. (B) Printed in negative image. From case MR-1. Sections are $60\ \mu\text{m}$ apart. CN, caudate nucleus; P, putamen; IC, internal capsule; NA, nucleus accumbens. (Bar = 1 mm.)

DISCUSSION

These observations have implications of at least two types. First, the findings indicate that pharmacologic treatments affecting the dopamine uptake mechanism may have differential effects on the striosome and matrix subdivisions of the dorsal striatum and on distinct subdivisions of the ventral striatum. Second, the findings suggest that entry of potential toxins into dopamine-containing fibers in the striatum could be different for these striatal compartments.

For the dorsal striatum the differences in $[^3\text{H}]$ mazindol binding were clearest in the caudate nucleus and, among species, were sharpest in the cat and only occasionally detectable, and then only ventrally, in the rat's caudoputamen. The lower numbers of uptake sites available for the binding of $[^3\text{H}]$ mazindol in striosomes suggest that there either are fewer dopamine-containing terminals in this striatal compartment or are fewer sites per terminal in striosomes than in the extrastriosomal matrix, or, conceivably, that the sites in the two striatal compartments have different molecular conformations although both bind $[^3\text{H}]$ mazindol. There is no direct evidence yet to settle this issue. Both striosomes and matrix are richly innervated by fibers from the midbrain, but different cell groups within the nigral complex innervate the two striatal compartments to different extents (18–20). Striosomes have lower tyrosine hydroxylase-like immunoreactivity than the extrastriosomal matrix (21, 22). This distinction, like that for the $[^3\text{H}]$ mazindol binding reported here, could reflect metabolic differences between striosome-directed and matrix-directed fibers rather than differences in the respective densities of such fibers. Olson *et al.* (23) have proposed such metabolic differences on the basis of experiments with tyrosine hydroxylase inhibitors.

The compartmental selectivity in $[^3\text{H}]$ mazindol binding in the caudate nucleus documented here provides additional evidence for fundamental differences between dopaminergic mechanisms in striosomes and matrix as judged not only by D1-selective ligand binding [heightened in striosomes (24)] and

D2-selective ligand binding [heightened in the matrix (25)] but also by presynaptic markers. Interestingly, all of these markers display greater compartmental selectivity in the caudate nucleus than in the putamen and are not as clearly compartmental in distribution in the rat (if they are at all) as they are in carnivores and primates. Amphetamine treatment in the rat has, however, been found to induce patchy anatomical distributions of transmitter-related compounds, including (presynaptic) tyrosine hydroxylase-immunoreactive patches (26) and (postsynaptic) dynorphin immunoreactive patches (27).

If synaptic release of dopamine is mainly from the newly synthesized pool of transmitter (28), the difference in number of uptake sites shown here for striosomes and matrix (about 50% maximum detected difference) might not be reflected functionally in these normally slow-firing neurons. Clearly, however, with intense firing and transmitter release or under the influence of drugs inducing massive transmitter release, differences in the capacity for transmitter clearance by re-uptake could be functionally significant. Uptake-site blockade by agents such as cocaine could also have markedly different effects on striosomes and matrix. Interpretation of such differences is now constrained by lack of information about the distribution of uptake sites on single terminals in striosomes and matrix; but given that the $[^3\text{H}]$ mazindol binding site has been directly related to the $[^3\text{H}]$ cocaine binding site on the dopamine uptake-site complex (2), the present results suggest that striosome–matrix differences in uptake-site distribution should be taken into account in addition to compartmental differences in D1/D2-binding-site ratios in analyzing drug effects on the nigrostriatal system.

There are considerable dose–response differences in the behavioral effects of drugs affecting catecholamine uptake sites, and some of these relate to the different expression of behaviors thought to be mediated preferentially by sensory–motor and limbic–hypothalamic mechanisms (2, 29, 30). The contrasting pre- and postsynaptic character of the dopamine innervations of striosomes and matrix could be essential to an understanding of these drug effects, for striosomes are preferentially related to a subset of limbic pathways and project to the substantia nigra, whereas the extrastriosomal matrix is linked to sensorimotor regions and other limbic pathways and projects preferentially into pallidum and nigrothalamic pathways (for review, see ref. 31).

For the dopamine-containing mesolimbic system, there also were striking regional inhomogeneities in uptake-site distribution, and these regional differences were at least as marked as those for striosomes and matrix in the dorsal striatum. Marshall (32) has already noted lower levels of $[^3\text{H}]$ dopamine uptake and $[^3\text{H}]$ mazindol binding in the ventral than in the dorsal striatum in the rat, and the present findings extend his observations by suggesting that different parts of the nucleus accumbens have different levels of $[^3\text{H}]$ mazindol binding. Selective functional effects of drugs would be ex-

Table 1. Densitometry on $[^3\text{H}]$ mazindol binding in the caudate nucleus of the cat

Section	$[^3\text{H}]$ Mazindol bound, Ci/mg of tissue		Striosome/ matrix ratio, %
	Striosome	Matrix	
763	10.60 \pm 2.69* (10)	22.71 \pm 2.30 (8)	46.7
643	13.66 \pm 1.98* (8)	22.45 \pm 3.06 (5)	60.8
715	10.60 \pm 2.69* (10)	22.70 \pm 2.30 (8)	46.7
571	11.85 \pm 3.91* (6)	22.67 \pm 2.63 (6)	52.2
Total	11.73 \pm 3.36 (34)	22.89 \pm 3.55 (29)	51.23

Higher section numbers are for more rostral sections. Values for $[^3\text{H}]$ mazindol binding to striosome and matrix are mean \pm SD. Numbers in parenthesis refer to *n*.

*Significantly different from binding in matrix at $P < 0.0001$.

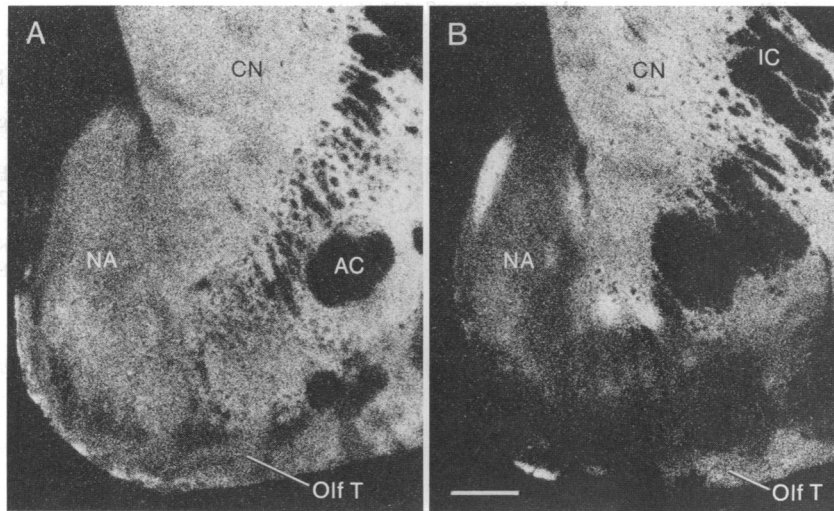


FIG. 4. Transverse sections at rostral (A) and caudal (B) levels through the ventral striatum of the cat illustrating the strong [^3H]mazindol binding in anterior and lateral parts of the nucleus accumbens and olfactory tubercle and the weak binding in caudal and medial parts of the ventral striatum. The sections were approximately $960\ \mu\text{m}$ apart. From case CDAR-4. Photographs were printed directly from the autoradiographic film. NA, nucleus accumbens; Olf T, olfactory tubercle; CN, caudate nucleus; IC, internal capsule; AC, anterior commissure. (Bar = 1 mm.)

pected according to these differences as well (see refs. 17 and 33). As in the dorsal striatum, there is no obvious relation between the degree of [^3H]mazindol binding and known intensities of total innervation by dopamine-containing fibers; for example, the dopamine-containing innervation is intense in the medial "shell" of the nucleus (17), where [^3H]mazindol binding is relatively weak.

The present observations have special significance in suggesting that different subdivisions of the nigrostriatal and mesolimbic systems might have different vulnerabilities to MPTP intoxication. In fact, there is a striking similarity between the striosomal patterning of [^3H]mazindol binding shown here for the cat and the pattern of fiber degeneration observed by Wilson *et al.* (34) and Turner *et al.* (35) in dogs acutely exposed to MPTP. At 8–14 days after MPTP injection, these authors found intense degeneration of fibers in the extrastriosomal matrix with relative sparing of fibers in the striosomes. They also describe the striosomal pattern as being clearest in the caudate nucleus at rostral and midanterior levels and illustrate fiber degeneration in the nucleus accumbens mainly in the lateral rather than the medial part of the nucleus.

Given the findings presented here, serious consideration should be given to the possibility that such differential patterns of MPTP-induced fiber degeneration might reflect local inhomogeneities in uptake-site distribution within the striatum, just as, in general, the greater vulnerability of more dorsal than more ventral striatal regions might be related to gradients of uptake-site distribution (27). The possibility that local variations in uptake-site distribution within the striatum constrain the level of degeneration induced by acute exposure to MPTP is in accord with the finding that intrastriatal administration of MPTP can induce degenerative changes in neurons in the midbrain (36, 37). Such differential vulnerability of fiber terminals could account for patterns of partial sparing of midbrain neurons seen with dose schedules producing submaximal damage to the system (38, 39). To the extent that the MPTP model relates to other forms of parkinsonism, the compartmental distributions of uptake sites described here could be important in constraining patterns of mesencephalic neuronal loss in these disorders as well (40).

It is a pleasure to thank Mr. Glenn Holm, Mrs. Yona Dornay, and Mrs. Judy Rankin for their technical support, Dr. Ann Kelley for reading the manuscript, Mr. Henry F. Hall, who is responsible for the photography, and Dr. William Houlihan of the Sandoz Research Institute for the gift of nonradioactive mazindol (Sanorex). This work was funded by Grant NS25529-02 (Javits Neuroscience Investigator Award) from the National Institutes of Health, the National Alliance for Research on Schizophrenia and Depression, the Scottish Rite Schizophrenia Research Program, The Seaver Institute, and the

National Parkinson Foundation. R.M. is a recipient of a fellowship from Consejo Superior de Investigaciones Científicas (Spain).

- Kennedy, L. T. & Hanbauer, I. (1983) *J. Neurochem.* **41**, 172–178.
- Ritz, M. C., Lamb, R. J., Goldberg, S. R. & Kuhar, M. J. (1987) *Science* **237**, 1219–1223.
- Heikkila, R. E., Cabbat, F. S. & Duvoisin, R. C. (1979) *Commun. Psychopharmacol.* **3**, 285–290.
- Davis, G. G., Williams, A. G., Markey, S. P., Ebert, M. H., Calne, C. D., Reichert, C. M. & Kopin, I. J. (1979) *Psychiatry Res.* **1**, 249–254.
- Burns, R. S., Chiueh, C. C., Markey, S. P., Ebert, M. H., Jacobowitz, D. M. & Kopin, I. J. (1983) *Proc. Natl. Acad. Sci. USA* **80**, 4546–4550.
- Langston, J. W., Ballard, P., Tetrud, J. W. & Irwin, I. (1983) *Science* **219**, 979–980.
- Chiba, K., Trevor, A. J. & Castagnoli, N., Jr. (1985) *Biochem. Biophys. Res. Commun.* **128**, 1228–1232.
- Javitch, J. A., D'Amato, R. J., Strittmatter, S. M. & Snyder, S. H. (1985) *Proc. Natl. Acad. Sci. USA* **82**, 2173–2177.
- Pileblad, E. & Carlsson, A. (1985) *Neuropharmacology* **24**, 689–692.
- Sundström, E., Goldstein, M. & Jonsson, G. (1986) *Eur. J. Pharmacol.* **131**, 289–292.
- Ricaurte, G. A., Langston, J. W., DeLanney, L. E., Irwin, I. & Brooks, J. D. (1985) *Neurosci. Lett.* **59**, 259–264.
- Schultz, W., Scarmatai, E., Sundström, E., Tsutsumi, T. & Jonsson, G. (1986) *Exp. Brain Res.* **63**, 216–220.
- Javitch, J. A., Strittmatter, S. M. & Snyder, S. H. (1985) *J. Neurosci.* **5**, 1513–1521.
- O'Dell, S. J. & Marshall, J. F. (1988) *Brain Res.* **460**, 402–406.
- Graybiel, A. M. & Ragsdale, C. W. (1978) *Proc. Natl. Acad. Sci. USA* **75**, 5723–5726.
- Geneser-Jensen, F. A. & Blackstad, J. W. (1971) *Z. Zellforsch. Mikrosk. Anat.* **114**, 460–481.
- Groenewegen, H. J., Meredith, G. E., Berendse, H. W., Voorn, P. & Wolters, J. G. (1989) in *Neural Mechanisms in Disorders of Movement*, eds. Crossman, A. & Sambrook, M. A. (Libbey, London), pp. 45–54.
- Jimenez-Castellanos, J. & Graybiel, A. M. (1987) *Neuroscience* **23**, 223–242.
- Gerfen, C. R., Herkenham, M. & Thibault, J. (1987) *J. Neurosci.* **7**, 3915–3934.
- Langer, L. F. & Graybiel, A. M. (1989) *Brain Res.* **498**, 344–350.
- Graybiel, A. M., Hirsch, E. C. & Agid, Y. A. (1987) *Proc. Natl. Acad. Sci. USA* **84**, 303–307.
- Ferrante, R. J. & Kowall, N. W. (1987) *Brain Res.* **416**, 141–146.
- Olson, L., Seiger, A. & Fuxe, K. (1972) *Brain Res.* **44**, 283–288.
- Besson, M.-J., Graybiel, A. M. & Nastuk, M. A. (1988) *Neuroscience* **26**, 101–119.
- Joyce, J. N., Sapp, D. W. & Marshall, J. F. (1986) *Proc. Natl. Acad. Sci. USA* **83**, 8002–8006.
- Ryan, L. J., Martone, M. E., Linder, J. C. & Groves, P. M.

- (1988) *Brain Res. Bull.* **21**, 133–137.
27. Li, S. J., Sivam, S. P., McGinty, J. F., Jiang, H. K., Douglass, J., Calavetta, L. & Hong, J. S. (1988) *J. Pharmacol. Exp. Ther.* **246**, 403–408.
28. Shore, P. A., McMillen, B. A., Miller, H. H., Sanghera, M. K., Kiser, R. S. & German, D. C. (1979) in *Catecholamines: Basic and Clinical Frontiers*, eds. Usdin, E., Kopin, I. J. & Barchas, J. (Pergamon, New York), pp. 722–727.
29. Kelly, P. H., Seviour, P. W. & Iversen, S. D. (1975) *Brain Res.* **94**, 507–522.
30. Kelley, A. E. & Gauthier, A. M. (1987) *Soc. Neurosci. Abstr.* **13**, 31.
31. Graybiel, A. M. (1989) in *Neural Mechanisms in Disorders of Movement*, eds. Crossman, A. & Sambrook, M. A. (Libbey, London), pp. 3–15.
32. Marshall, J. F. (1988) *Soc. Neurosci. Abstr.* **14**, 157.
33. Kelley, A. E., Domesick, V. B. & Nauta, W. J. H. (1982) *Neuroscience* **7**, 615–630.
34. Wilson, J. S., Turner, B. H., Morrow, G. D. & Hartman, P. J. (1987) *Brain Res.* **423**, 329–332.
35. Turner, B. H., Wilson, J. S., McKenzie, J. C. & Richtand, N. (1988) *Brain Res.* **473**, 60–64.
36. Imai, H., Nakamura, T., Endo, K. & Narabayashi, H. (1988) *Brain Res.* **474**, 327–332.
37. Bradbury, A. J., Costall, B., Jenner, P. C., Kelly, M. E., Marsden, C. E. & Naylor, R. J. (1986) *Neuropharmacology* **25**, 939–941.
38. Deutch, A. Y., Elsworth, J. D., Goldstein, M., Fuxe, K., Redmond, D. E., Jr., Sladek, J. R., Jr., & Roth, R. H. (1986) *Neurosci. Lett.* **68**, 51–56.
39. German, D. C., Dubach, M., Askari, S., Speciale, S. G. & Bowden, D. M. (1988) *Neuroscience* **24**, 161–174.
40. Graybiel, A. M., Hirsch, E. C. & Agid, Y. (1989) in *Ninth International Symposium on Parkinson's Disease*, in press.